Science and Technology Infusion Climate Bulletin
NOAA's National Weather Service
41st NOAA Annual Climate Diagnostics and Prediction Workshop
Orono, ME, 3-6 October 2016

A Process-based Attribution of the Difference in the Annual Variation of Surface Temperature between the Monsoon and Non-monsoon Regions

Yana Li[1], Song Yang[1], Yi Deng[2] and Xiaoming Hu[1]
[1]*School of Atmospheric Sciences, Sun Yat-sen University, Guangzhou, China*
[2]*School of Earth and Atmospheric Sciences, Georgia Institute of Technology, Atlanta*

1. Data and methodology

The primary dataset used is the European Centre for Medium-Range Weather Forecasts (ECMWF) Re-Analysis Interim (ERA-Interim, Uppala *et al.* 2008; Dee *et al.* 2011) covering the period of 1979 to present with a horizontal resolution of 1° longitude × 1° latitude and 37 pressure levels in the vertical ranging from 1000 hPa to 1 hPa.

We have adopted the same package of a climate feedback-response analysis method (CFRAM), which is based on the total energy balance within an atmosphere-surface column at a given horizontal grid point that consists of M atmospheric layers and a surface layer (Cai and Lu, 2009; Lu and Cai, 2009). Following Deng *et al.* (2012), we write the total energy balance equation separately for a month (*i.e.* March) and its latter month (*i.e.* April), take the difference (Δ) between the two months (*e.g.* April-March), and we obtain

$$\Delta\frac{\partial E}{\partial t} = \Delta S - \Delta R + \Delta Q^{non-radiative} \quad (1)$$

where R (S) is the vertical profile of the net convergence (divergence) of short-wave (long-wave) radiation flux within each layer. For all layers above the surface, $\Delta Q^{non-radiative}$ is the vertical profile of the convergence of total energy due to atmospheric turbulent, convective, and advective motions.

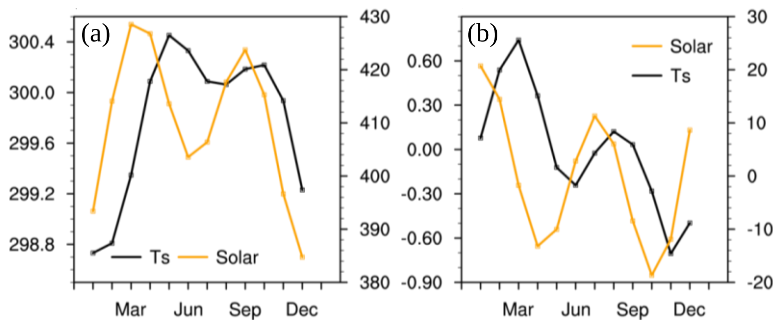

Fig. 1 (a) Climatology of annual variations of the solar radiation at the top of troposphere (TOA) (yellow solid line, corresponding to the right Y-axis, unit: W/m**2) and the surface temperature (black solid line, corresponding to the left Y-axis, unit: K) average over the monsoon region (15°S-15°N, 105°-150°E). (b) The increment between two months of the solar radiation (yellow solid line) and the surface temperature (the black solid line), and the corresponding Y-axis is same as in (a).

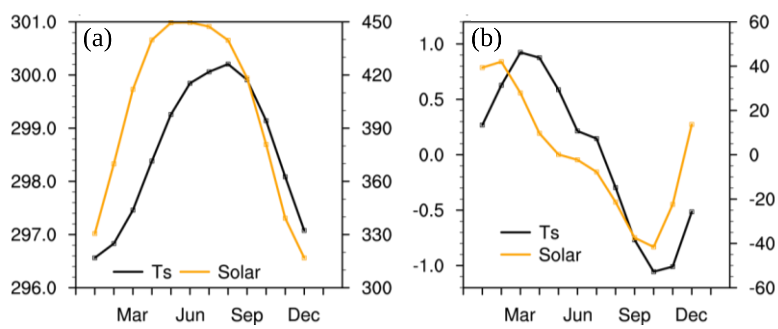

Fig. 2 Same as Fig. 1, but for the non-monsoon region (5°N-30°N, 260°-300°E).

By neglecting the interactions among various radiative feedback processes thus linearizing the radiative energy perturbation, following Hu et al. (2016), we may express ΔS and ΔR as

$$\Delta S \approx \Delta S^{solar} + \Delta S^{wv} + \Delta S^{c} + \Delta S^{\alpha} \text{ and } \Delta R \approx \Delta R^{wv} + \Delta R^{c} + \frac{\partial R}{\partial T}\Delta T \quad (2)$$

In Eq. (2), superscripts, "solar", "wv", "c", and "α", indicate solar insolation, water vapor, cloud, and surface albedo, respectively. Elements of ΔT are the vertical profile of temperature differences in each layer between months, and ∂R/∂T is the Planck feedback matrix. Substituting Eq. (2) into Eq. (1), we obtain,

Correspondence to: Yana Li, School of Atmospheric Sciences, Sun Yat-sen University, Guangzhou, China;
E-mail: liyana@mail2.sysu.edu.cn

$$\Delta T = \left(\frac{\partial R}{\partial T}\right)^{-1}\left\{\Delta S^{solar} + \Delta(S-R)^{wv} + \Delta(S-R)^{c} + \Delta S^{\alpha} + \Delta Q^{atmos\_dyn} + \Delta Q^{surface}\right\} \quad (3)$$

From (3), we can separate the temperature change between two months, for example, March-to-April, to all the dynamical and thermodynamical processes.

Additionally, a temporal pattern-amplitude projection (TPAP) method, is applied to quantify the relative contribution of each process annual variaiton to the annual cycle of observations,

$$TPAP_i = \frac{\sum_1^{12}(\Delta T_{in} * \Delta T_n)}{\sum_1^{12}(\Delta T_n)^2} \quad (5)$$

where i and n refer to the ith feedback process and nth month from January to December, and ΔT is the observation.

2. Results

The South China Sea (SCS) and the southern North America (SNA) are representative of the monsoon and non-monsoon regions, respectively. The annual variation of areal average surface temperature in SCS is bimodal (Fig. 1a), and that in SNA peaks at August (Fig. 2a). The rapid warming month over both regions is March to April (Fig. 1b and Fig. 2b).

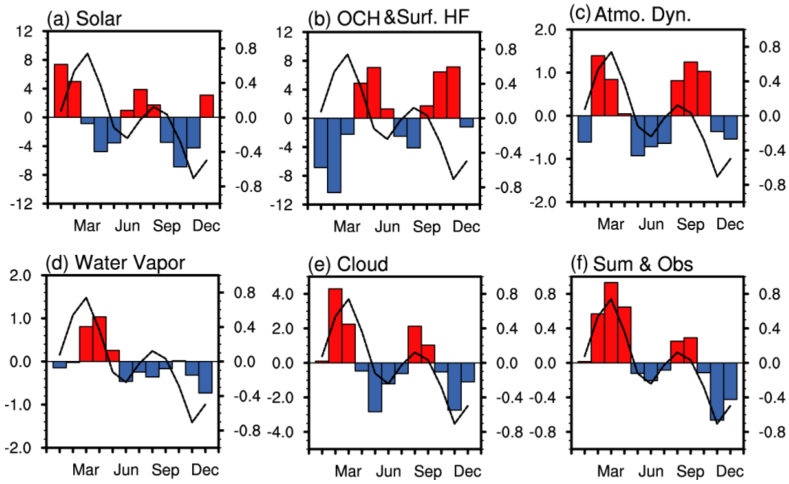

Fig. 3 Annual cycle of partial temperature changes (K) of surface temperature average over (15°S-25°N, 105°-150°E) due to changes in (a) solar radiation at the TOA, (b) oceanic dynamic and ocean/land heat storage (OCH) and surface heat flux, (c) the atmospheric dynamics, (d) water vapor, (e) cloud, (f) sum of all individual feedback processes. The black solid lines in (a-f) refer to the observation (K).

For the monsoon region, main positive contributors to the annual variation of surface temperature are the quick feedback processes in the atmosphere such as the changes in cloud cover, water vapor and atmospheric dynamics, while the incident solar radiation at the top of the atmosphere, and the oceanic dynamical processes with the land/ocean heat storage are two greatest factors, from the perspective of contribution magnitude (Fig. 3 and Fig. 5a).

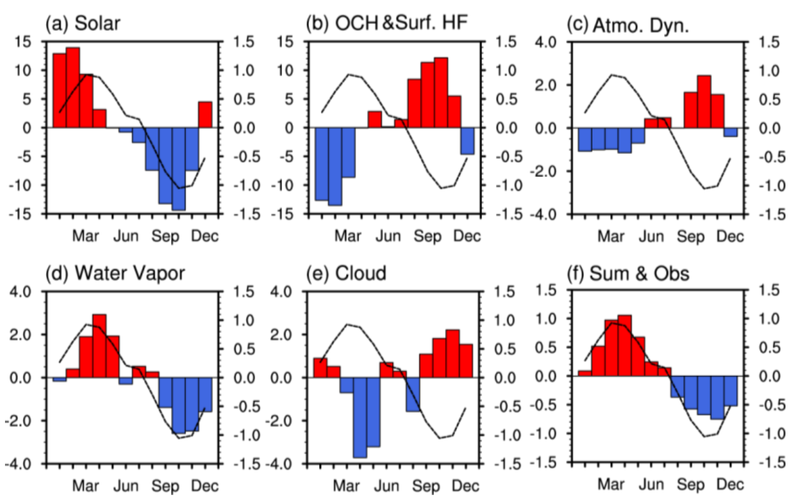

Fig. 4 Same as Fig. 3, but for the non-monsoon region (5°N-30°N, 260°-300°E).

For non-monsoon regions, the main contributor for the annual cycle of surface temperature is solar insolation. The quick feedback processed in the atmosphere contributes little, only water vapor contributing positively (Fig. 4 and Fig. 5b). Ocean is the largest negative contributor in both monsoon and non-monsoon regions, which delays the direct effect of solar radiation on the surface temperature. However, more enhanced air-sea interaction in monsoon region counteracts the oceanic negative contribution by the positive contribution of surface latent heat flux.

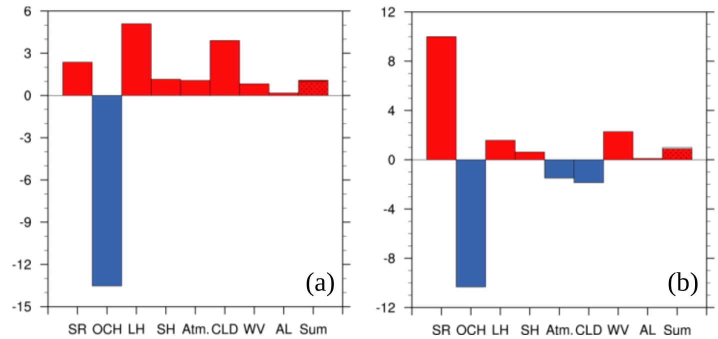

Fig. 5 Temporal pattern-amplitude projection coefficients (TPAPs) associated with each radiative and non-radiative forcing of the areal averaged surface anomalies over (a) (15°S-25°N, 105°-150°E) and (b) (5°N-30°N, 260°-300°E). The box with black dots over "Sum" refers to the observation.

References

Cai, M, and J.-H. Lu, 2009: A new framework for isolating individual feedback processes in coupled general circulation climate models. Part II: method demonstrations and comparisons. *Clim. Dyn.*, **32**, 887-900.

Dee, D.P., and Coauthors, 2011: The ERA-Interim reanalysis: configuration and performance of the data assimilation system. *Q. J. Roy. Meteor. Soc.*, **137,** 553-597.

Deng, Y., T.W. Park, and M. Cai, 2012: Process-based decomposition of the global surface temperature response to El Niño in boreal winter. *J. Atmos. Sci.*, **69**, 1706–1712.

Hu, X.M., S. Yang, and M. Cai, 2016: Contrasting the eastern Pacific El Niño and the central Pacific El Niño: Process-based feedback attribution. *Clim. Dyn.*, **47**, 2413. doi: 10.1007/s00382-015-2971-9.

Lu, J.H., and M. Cai, 2009: A new framework for isolating individual feedback process in coupled general circulation climate models. Part I: Formulation. *Clim. Dyn.*, **32**, 873-885.

Uppala S.M., D. Dee, S. Kobayashi, P. Berrisford, and A. Simmons, 2008: Towards a climate data-assimilation system: Status update of ERA–Interim. *ECMWF Newletter*, **115**, 12-18.